two phases can also be expressed using the activity concept defined for homogeneous systems in Fig. 1.16. In heterogeneous systems containing more than one phase the pure components can, at least theoretically, exist in different crystal structures. The most stable state, with the lowest free energy, is usually defined as the state in which the pure component has unit activity. In the present example this would correspond to defining the activity of A in pure α – A as unity, i.e. when $X_A = 1$, $a_A^\alpha = 1$. Similarly when $X_B = 1$, $a_B^\beta = 1$. This definition of activity is shown graphically in Fig. 1.28a; Fig. 1.28b and c show how the activities of B and A vary with the composition of the α and β phases. Between A and α_e, and β_e and B, where single phases are stable, the activities (or chemical potentials) vary and for simplicity ideal solutions have been assumed in which case there is a straight line relationship between a and X. Between α_e and β_e the phase compositions in equilibrium do not change and the activities are equal and given by points q and r. In other words, when two phases exist in equilibrium, the activities of the components in the system must be equal in the two phases, i.e.

$$a_A^\alpha = a_A^\beta, \qquad a_B^\alpha = a_B^\beta \tag{1.47}$$

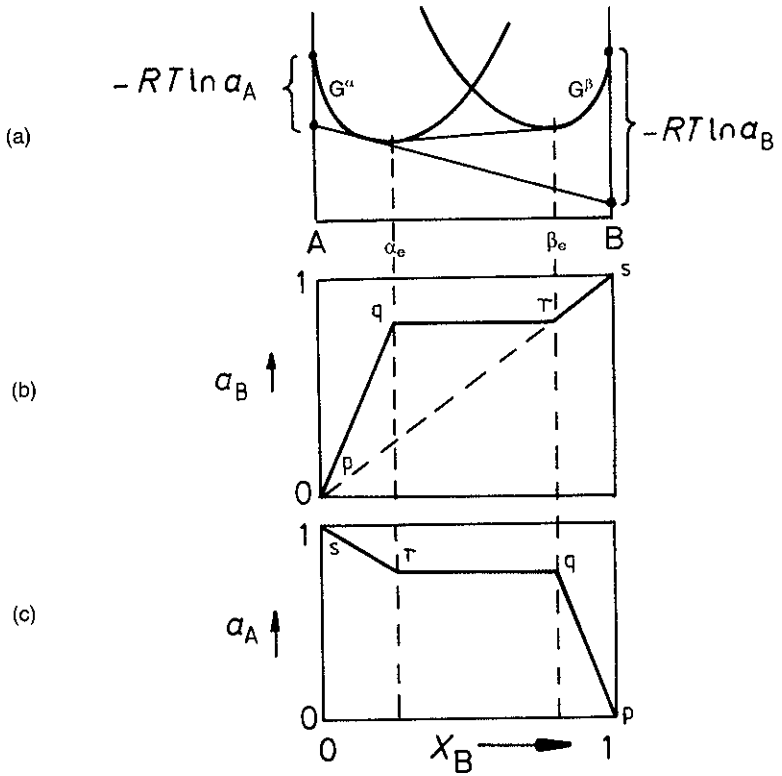

Fig. 1.28 The variation of a_A and a_B with composition for a binary system containing two ideal solutions, α and β.

1.5 Binary Phase Diagrams

In the previous section it has been shown how the equilibrium state of an alloy can be obtained from the free energy curves at a given temperature. The next step is to see how equilibrium is affected by temperature.

1.5.1 A Simple Phase Diagram

The simplest case to start with is when A and B are completely miscible in both the solid and liquid states and both are ideal solutions. The free energy of pure A and pure B will vary with temperature as shown schematically in Fig. 1.4. The equilibrium melting temperatures of the pure components occur when $G^S = G^L$, i.e. at $T_m(A)$ and $T_m(B)$. The free energy of both phases decreases as temperature increases. These variations are important for A–B alloys also since they determine the relative positions of G_A^S, G_A^L, G_B^S and G_B^L on the molar free energy diagrams of the alloy at different temperatures, Fig. 1.29.

At a high temperature $T_1 > T_m(A) > T_m(B)$ the liquid will be the stable phase for pure A and pure B, and for the simple case we are considering the liquid also has a lower free energy than the solid at all the intermediate compositions as shown in Fig. 1.29a.

Decreasing the temperature will have two effects: firstly G_A^L and G_B^L will increase more rapidly than G_A^S and G_B^S, secondly the curvature of the G curves will be reduced due to the smaller contribution of $-T\Delta S_{mix}$ to the free energy.

At $T_m(A)$, Fig. 1.29b, $G_A^S = G_A^L$, and this corresponds to point a on the A–B phase diagram, Fig. 1.29f. At a lower temperature T_2 the free energy curves cross, Fig. 1.29c, and the common tangent construction indicates that alloys between A and b are solid at equilibrium, between c and B they are liquid, and between b and c equilibrium consists of a two-phase mixture (S + L) with compositions b and c. These points are plotted on the equilibrium phase diagram at T_2.

Between T_2 and $T_m(B)$ G^L continues to rise faster than G^S so that points b and c in Fig. 1.29c will both move to the right tracing out the solidus and liquidus lines in the phase diagram. Eventually at $T_m(B)$ b and c will meet at a single point, d in Fig. 1.29f. Below $T_m(B)$ the free energy of the solid phase is everywhere below that of the liquid and all alloys are stable as a single phase solid.

1.5.2 Systems with a Miscibility Gap

Figure 1.30 shows the free energy curves for a system in which the liquid phase is approximately ideal, but for the solid phase $\Delta H_{mix} > 0$, i.e. the A and B atoms 'dislike' each other. Therefore at low temperatures (T_3) the free energy curve for the solid assumes a negative curvature in the middle,

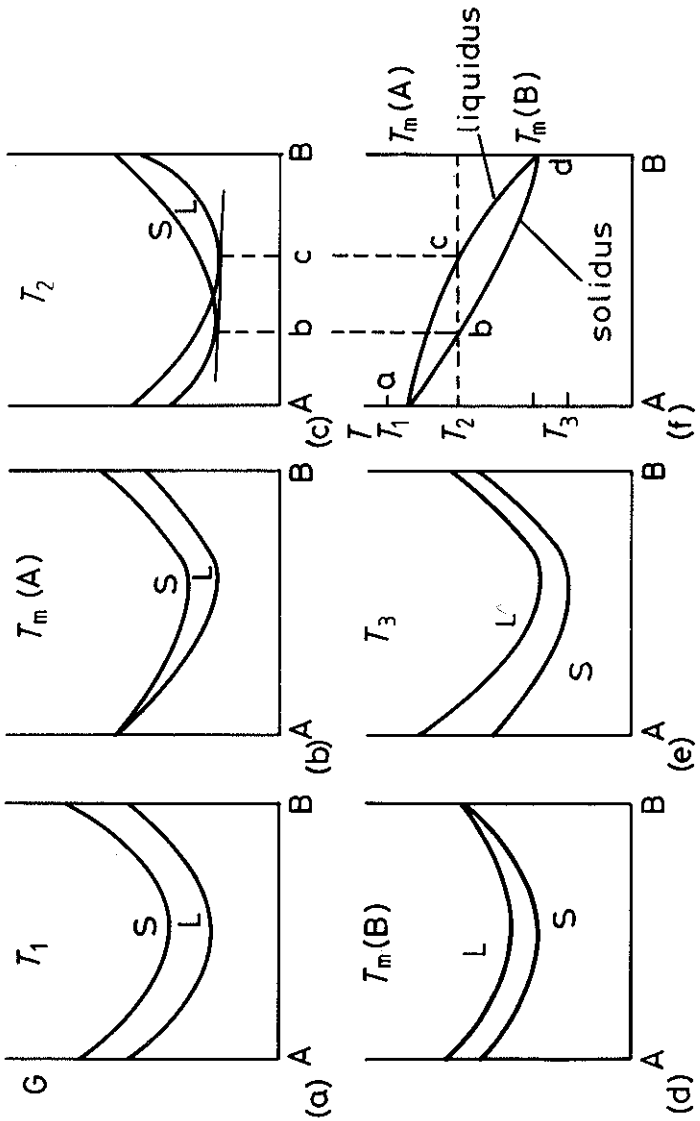

Fig. 1.29 The derivation of a simple phase diagram from the free energy curves for the liquid (L) and solid (S).

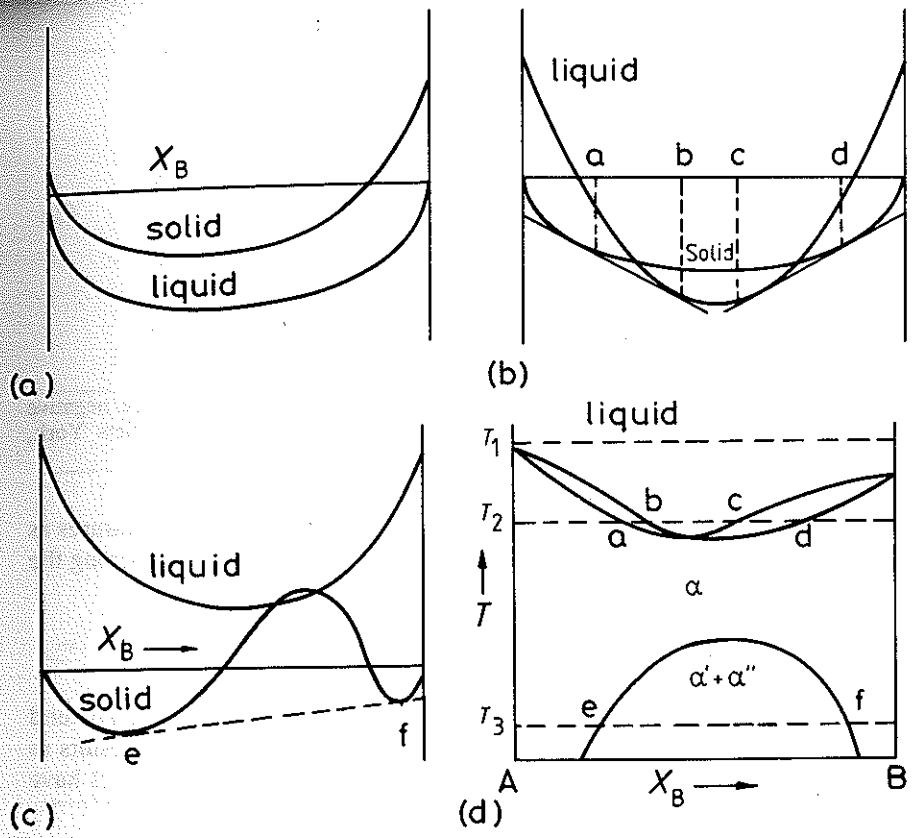

Fig. 1.30 The derivation of a phase diagram where $\Delta H^{S}_{mix} > \Delta H^{L}_{mix} = 0$. Free energy v. composition curves for (a) T_1, (b) T_2, and (c) T_3.

Fig. 1.30c, and the solid solution is most stable as a mixture of two phases α′ and α″ with compositions e and f. At higher temperatures, when $-T\Delta S_{mix}$ becomes larger, e and f approach each other and eventually disappear as shown in the phase diagram, Fig. 1.30d. The α′ + α″ region is known as a miscibility gap.

The effect of a positive ΔH_{mix} in the solid is already apparent at higher temperatures where it gives rise to a minimum melting point mixture. The reason why all alloys should melt at temperatures below the melting points of both components can be qualitatively understood since the atoms in the alloy 'repel' each other making the disruption of the solid into a liquid phase possible at lower temperatures than in either pure A or pure B.

1.5.3 Ordered Alloys

The opposite type of effect arises when $\Delta H_{mix} < 0$. In these systems melting will be more difficult in the alloys and a maximum melting point mixture may

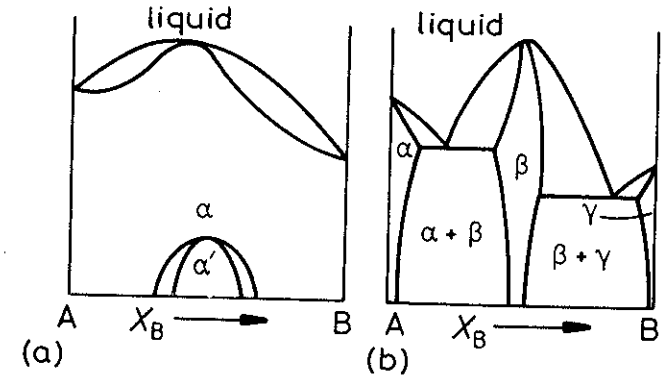

Fig. 1.31 (a) Phase diagram when $\Delta H^S_{mix} < 0$; (b) as (a) but even more negative ΔH^S_{mix}. (After R.A. Swalin, *Thermodynamics of Solids*, John Wiley, New York, 1972).

appear. This type of alloy also has a tendency to order at low temperatures as shown in Fig. 1.31a. If the attraction between unlike atoms is very strong the ordered phase may extend as far as the liquid, Fig. 1.31b.

1.5.4 Simple Eutectic Systems

If ΔH^S_{mix} is much larger than zero the miscibility gap in Fig. 1.30d can extend into the liquid phase. In this case a simple eutectic phase diagram results as shown in Fig. 1.32. A similar phase diagram can result when A and B have different crystal structures as illustrated in Fig. 1.33

1.5.5 Phase Diagrams Containing Intermediate Phases

When stable intermediate phases can form, extra free energy curves appear in the phase diagram. An example is shown in Fig. 1.34, which also illustrates how a peritectic transformation is related to the free energy curves.

An interesting result of the common tangent construction is that the stable composition range of the phase in the phase diagram need not include the composition with the minimum free energy, but is determined by the relative free energies of adjacent phases, Fig. 1.35. This can explain why the composition of the equilibrium phase appears to deviate from that which would be predicted from the crystal structure. For example the θ phase in the Cu–Al system is usually denoted as $CuAl_2$ although the composition $X_{Cu} = 1/3$, $X_{Al} = 2/3$ is not covered by the θ field on the phase diagram.

1.5.6 The Gibbs Phase Rule

The condition for equilibrium in a binary system containing two phases is given by Equation 1.46 or 1.47. A more general requirement for systems

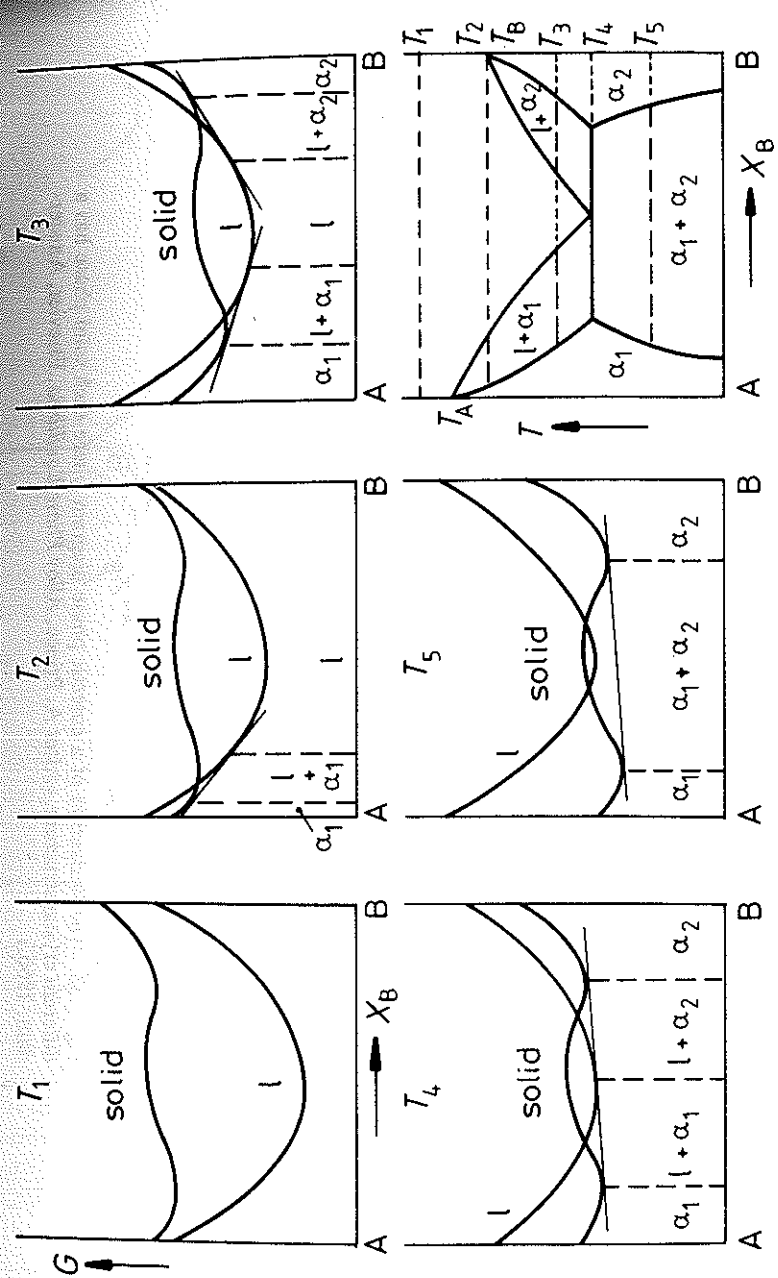

Fig. 1.32 The derivation of a eutectic phase diagram where both solid phases have the same crystal structure. (After A.H. Cottrell, *Theoretical Structural Metallurgy*, Edward Arnold, London, 1955, ©Sir Alan Cottrell.)

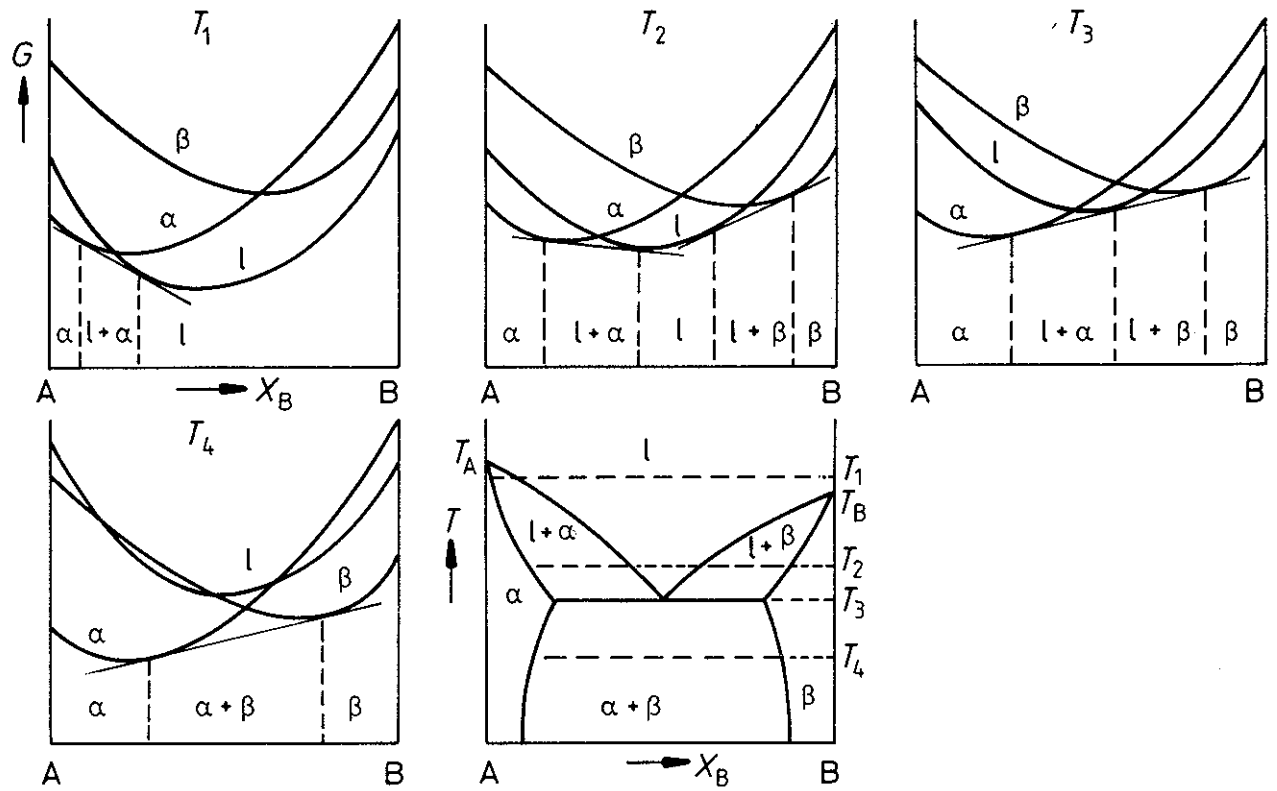

Fig. 1.33 The derivation of a eutectic phase diagram where each solid phase has a different crystal structure. (After A. Prince, *Alloy Phase Equilibria*, Elsevier, Amsterdam, 1966.)

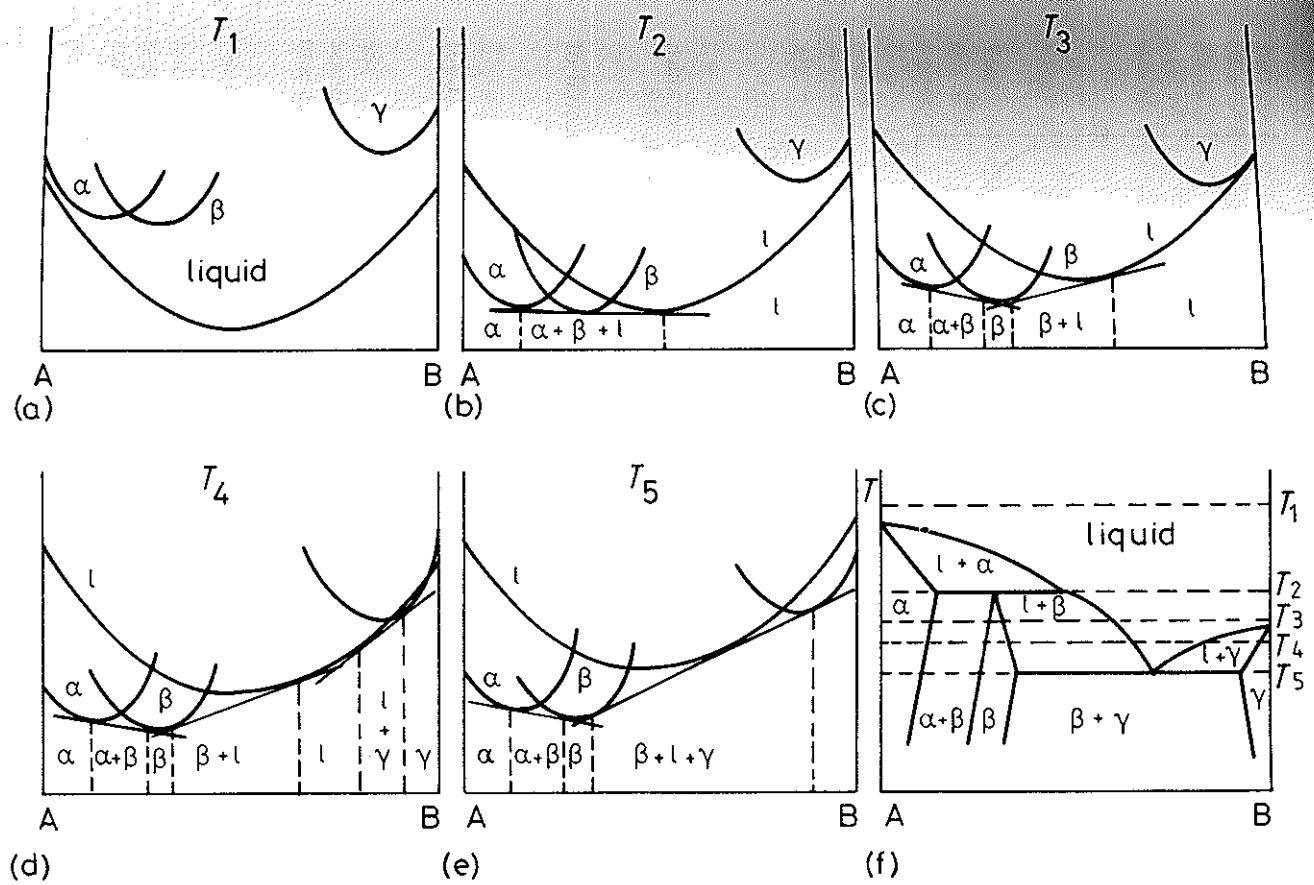

Fig. 1.34 The derivation of a complex phase diagram. (After A.H. Cottrell, *Theoretical Structural Metallurgy*, Edward Arnold, London, 1955, © Sir Alan Cottrell.)

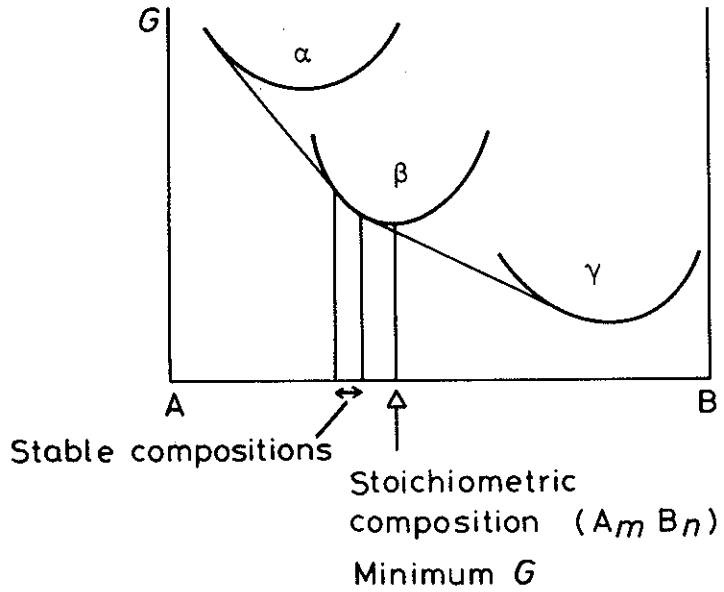

Fig. 1.35 Free energy diagram to illustrate that the range of compositions over which a phase is stable depends on the free energies of the other phases in equilibrium.

containing several components and phases is that the chemical potential of each component must be identical in every phase, i.e.

$$\begin{aligned} \mu_A^\alpha &= \mu_A^\beta = \mu_A^\gamma = \ldots \\ \mu_B^\alpha &= \mu_B^\beta = \mu_B^\gamma = \ldots \\ \mu_C^\alpha &= \mu_C^\beta = \mu_C^\gamma = \ldots \end{aligned} \tag{1.48}$$

The proof of this relationship is left as an exercise for the reader (see Exercise 1.10). A consequence of this general condition is the Gibbs phase rule. This states that if a system containing C components and P phases is in equilibrium the number of degrees of freedom F is given by

$$P + F = C + 2 \tag{1.49}$$

A degree of freedom is an intensive variable such as T, P, X_A, X_B . . . that can be varied independently while still maintaining equilibrium. If pressure is maintained constant one degree of freedom is lost and the phase rule becomes

$$P + F = C + 1 \tag{1.50}$$

At present we are considering binary alloys so that $C = 2$ therefore

$$P + F = 3$$

This means that a binary system containing one phase has two degrees of freedom, i.e. T and X_B can be varied independently. In a two-phase region of

a phase diagram $P = 2$ and therefore $F = 1$ which means that if the temperature is chosen independently the compositions of the phases are fixed. When three phases are in equilibrium, such as at a eutectic or peritectic temperature, there are no degrees of freedom and the compositions of the phases and the temperature of the system are all fixed.

1.5.7 The Effect of Temperature on Solid Solubility

The equations for free energy and chemical potential can be used to derive the effect of temperature on the limits of solid solubility in a terminal solid solution. Consider for simplicity the phase diagram shown in Fig. 1.36a where B is soluble in A, but A is virtually insoluble in B. The corresponding free energy curves for temperature T_1 are shown schematically in Fig. 1.36b. Since A is almost insoluble in B the G^β curve rises rapidly as shown. Therefore the maximum concentration of B soluble in A (X_B^e) is given by the condition

$$\mu_B^\alpha = \mu_B^\beta \simeq G_B^\beta$$

For a *regular solid solution* Equation 1.40 gives

$$\mu_B^\alpha = G_B^\alpha + \Omega(1 - X_B)^2 + RT \ln X_B$$

But from Fig. 1.36b, $G_B^\alpha - \mu_B^\alpha = \Delta G_B$, the difference in free energy between pure B in the stable β-form and the unstable α-form. Therefore for $X_B = X_B^e$

$$-RT \ln X_B^e - \Omega(1 - X_B^e)^2 = \Delta G_B \tag{1.51}$$

If the solubility is low $X_B^e \ll 1$ and this gives

$$X_B^e = \exp\left\{-\frac{\Delta G_B + \Omega}{RT}\right\} \tag{1.52}$$

Putting

$$\Delta G_B = \Delta H_B - T\Delta S_B$$

gives

$$X_B^e = A \exp \frac{-Q}{RT} \tag{1.53}$$

where A is a constant equal to $\exp(\Delta S_B/R)$ and

$$Q = \Delta H_B + \Omega \tag{1.54}$$

ΔH_B is the difference in enthalpy between the β-form of B and the α-form in J mol^{-1}. Ω is the change in energy when 1 mol of B with the α-structure dissolves in A to make a dilute solution. Therefore Q is just the enthalpy change, or heat absorbed, when 1 mol of B with the β-structure dissolves in A to make a dilute solution.

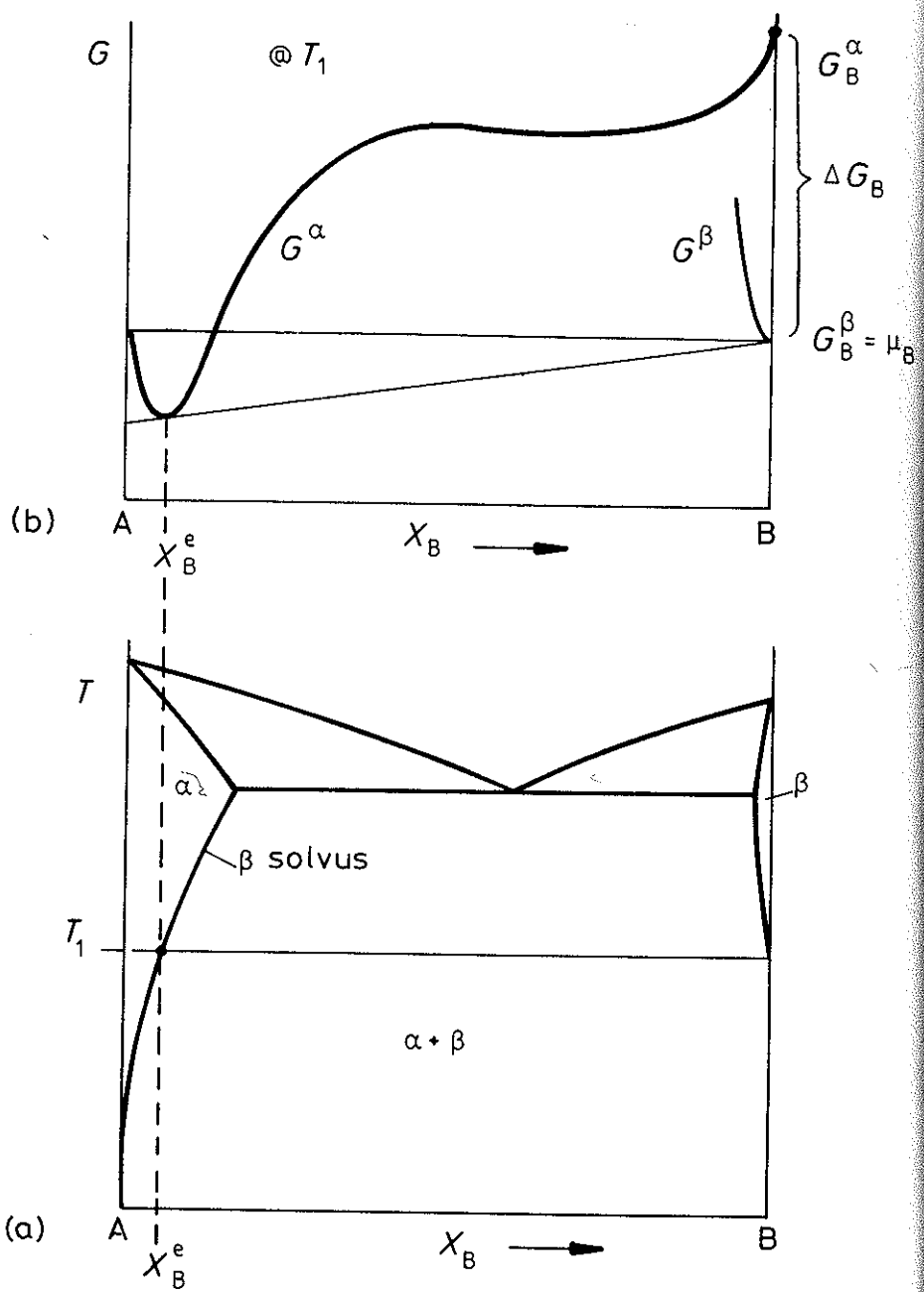

Fig. 1.36 Solubility of B in A.

ΔS_B is the difference in entropy between β-B and α-B and is approximately independent of temperature. Therefore the solubility of B in α increases exponentially with temperature at a rate determined by Q. It is interesting to note that, except at absolute zero, X_B^e can never be equal to zero, that is, no two components are ever completely insoluble in each other.

1.5.8 Equilibrium Vacancy Concentration

So far it has been assumed that in a metal lattice every atom site is occupied. However, let us now consider the possibility that some sites remain without atoms, that is, there are *vacancies* in the lattice. The removal of atoms from their sites not only increases the internal energy of the metal, due to the broken bonds around the vacancy, but also increases the randomness or configurational entropy of the system. The free energy of the alloy will depend on the concentration of vacancies and the equilibrium concentration X_v^e will be that which gives the minimum free energy.

If, for simplicity, we consider vacancies in a pure metal the problem of calculating X_v^e is almost identical to the calculation of ΔG_{mix} for A and B atoms when ΔH_{mix} is positive. Because the equilibrium concentration of vacancies is small the problem is simplified because vacancy–vacancy interactions can be ignored and the increase in enthalpy of the solid (ΔH) is directly proportional to the number of vacancies added, i.e.

$$\Delta H \simeq \Delta H_v X_v$$

where X_v is the mole fraction of vacancies and ΔH_v is the increase in enthalpy per mole of vacancies added. (Each vacancy causes an increase of $\Delta H_v/N_a$ where N_a is Avogadro's number.)

There are two contributions to the entropy change ΔS on adding vacancies. There is a small change in the thermal entropy of ΔS_v per mole of vacancies added due to changes in the vibrational frequencies of the atoms around a vacancy. The largest contribution, however, is due to the increase in configurational entropy given by Equation 1.25. The total entropy change is thus

$$\Delta S = X_v \Delta S_v - R(X_v \ln X_v + (1 - X_v) \ln (1 - X_v))$$

The molar free energy of the crystal containing X_v mol of vacancies is therefore given by

$$G = G_A + \Delta G = G_A + \Delta H_v X_v - T\Delta S_v X_v + RT(X_v \ln X_v + (1 - X_v) \ln (1 - X_v)) \qquad (1.55)$$

This is shown schematically in Fig. 1.37. Given time the number of vacancies will adjust so as to reduce G to a minimum. The equilibrium concentration of vacancies X_v^e is therefore given by the condition

$$\left.\frac{dG}{dX_v}\right|_{X_v = X_v^e} = 0$$

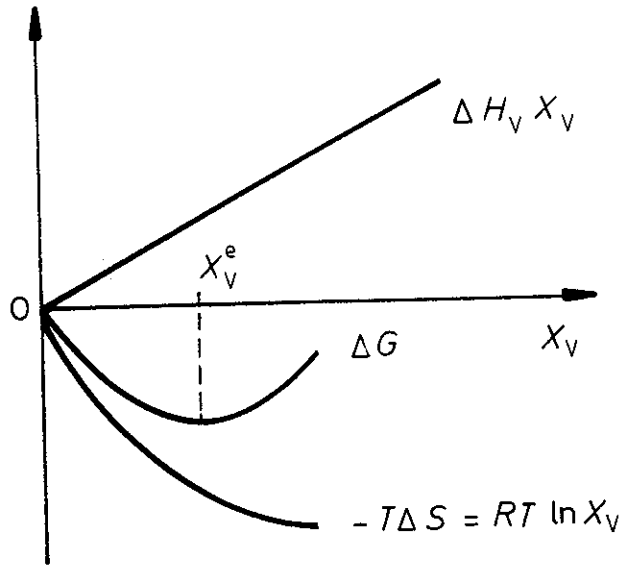

Fig. 1.37 Equilibrium vacancy concentration.

Differentiating Equation 1.55 and making the approximation $X_v \ll 1$ gives

$$\Delta H_v - T\Delta S_v + RT \ln X_v^e = 0$$

Therefore the expression for X_v^e is

$$X_v^e = \exp \frac{\Delta S_v}{R} \cdot \exp \frac{-\Delta H_v}{RT} \tag{1.56}$$

or, putting $\Delta G_v = \Delta H_v - T\Delta S_v$ gives

$$X_v^e = \exp \frac{-\Delta G_v}{RT} \tag{1.57}$$

The first term on the right-hand side of Equation 1.56 is a constant ~3, independent of T, whereas the second term increases rapidly with increasing T. In practice ΔH_v is of the order of 1 eV per atom and X_v^e reaches a value of about 10^{-4}–10^{-3} at the melting point of the solid.

1.6 The Influence of Interfaces on Equilibrium

The free energy curves that have been drawn so far have been based on the molar free energies of infinitely large amounts of material of a perfect single crystal. Surfaces, grain boundaries and interphase interfaces have been ignored. In real situations these and other crystal defects such as dislocations do exist and raise the free energies of the phases. Therefore the minimum free

energy of an alloy, i.e. the equilibrium state, is not reached until virtually all interfaces and dislocations have been annealed out. In practice such a state is unattainable within reasonable periods of time.

Interphase interfaces can become extremely important in the early stages of phase transformations when one phase, β, say, can be present as very fine particles in the other phase, α, as shown in Fig. 1.38a. If the α phase is acted on by a pressure of 1 atm the β phase is subjected to an extra pressure ΔP due to the curvature of the α/β interface, just as a soap bubble exerts an extra pressure ΔP on its contents. If γ is the α/β interfacial energy and the particles are spherical with a radius r, ΔP is given approximately by

$$\Delta P = \frac{2\gamma}{r}$$

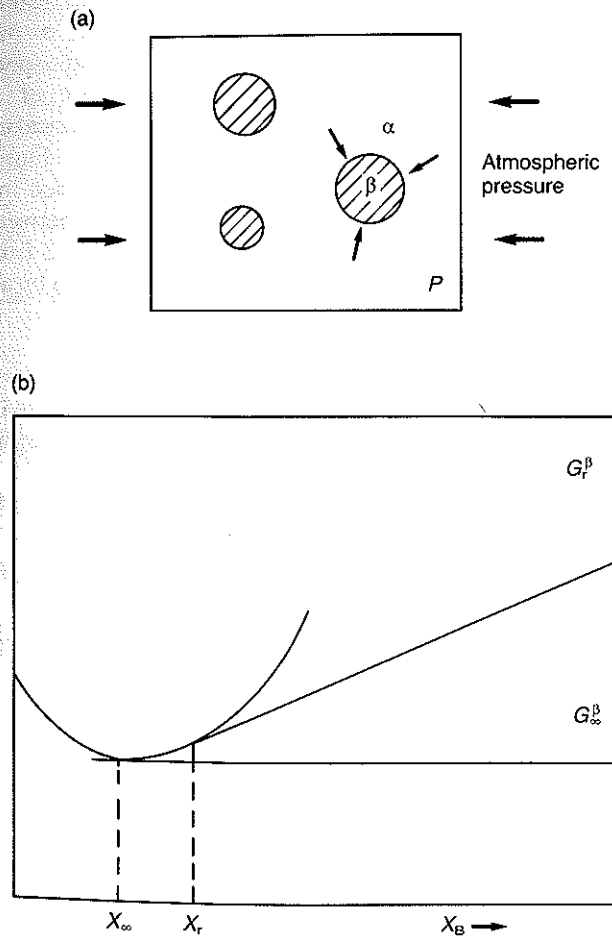

Fig. 1.38 The effect of interfacial energy on the solubility of small particles.

By definition, the Gibbs free energy contains a 'PV' term and an increase of pressure P therefore causes an increase in free energy G. From Equation 1.9 at constant temperature

$$\Delta G = \Delta P \cdot V$$

Therefore the β curve on the molar free energy–composition diagram in Fig. 1.38b will be raised by an amount

$$\Delta G_\gamma = \frac{2\gamma V_m}{r} \tag{1.58}$$

where V_m is the molar volume of the β phase. This free energy increase due to interfacial energy is known as a capillarity effect or the Gibbs–Thomson effect.

The concept of a pressure difference is very useful for spherical liquid particles, but it is less convenient in solids. This is because, as will be discussed in Chapter 3, finely dispersed solid phases are often non-spherical. For illustration, therefore, consider an alternative derivation of Equation 1.58 which can be more easily modified to deal with non-spherical cases[3].

Consider a system containing two β particles one with a spherical interface of radius r and the other with a planar interface ($r = \infty$) embedded in an α matrix as shown in Fig. 1.39. If the molar free energy difference between the two particles is ΔG_γ, the transfer of a small quantity (dn mol) of β from the large to the small particle will increase the free energy of the system by a small amount (dG) given by

$$dG = \Delta G_\gamma dn$$

If the surface area of the large particle remains unchanged the increase in free energy will be due to the increase in the interfacial area of the spherical

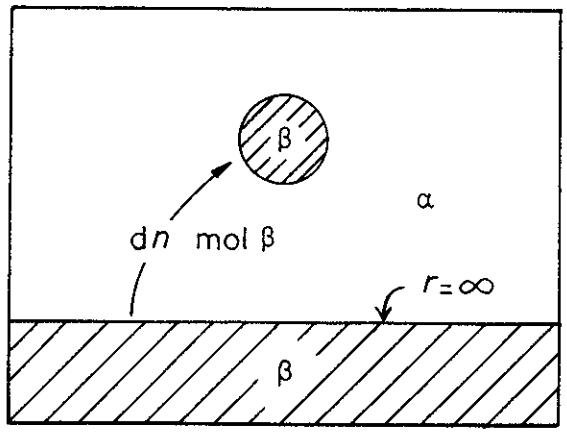

Fig. 1.39 Transfer of dn mol of β from large to a small particle.

particle (dA). Therefore assuming γ is constant

$$dG = \gamma dA$$

Equating these two expressions gives

$$\Delta G_\gamma = \gamma \frac{dA}{dn} \tag{1.59}$$

Since $n = 4\pi r^3/3V_m$ and $A = 4\pi r^2$ it can easily be shown that

$$\frac{dA}{dn} = \frac{dA/dr}{dn/dr} = \frac{2V_m}{r}$$

from which Equation 1.58 can be obtained.

An important practical consequence of the Gibbs–Thomson effect is that the solubility of β in α is sensitive to the size of the β particles. From the common tangent construction in Fig. 1.38b it can be seen that the concentration of solute B in α in equilibrium with β across a curved interface (X_r) is greater than X_∞, the equilibrium concentration for a planar interface. Assuming for simplicity that the α phase is a regular solution and that the β phase is almost pure B, i.e. $X_B^\beta \sim 1$, Equation 1.52 gives

$$X_\infty = \exp\left\{-\frac{\Delta G_B + \Omega}{RT}\right\}$$

Similarly X_r can be obtained by using $(\Delta G_B - 2\gamma V_m/r)$ in place of ΔG_B

$$X_r = \exp\left\{-\frac{\Delta G_B + \Omega - 2\gamma V_m/r}{RT}\right\}$$

Therefore

$$X_r = X_\infty \exp\frac{2\gamma V_m}{RTr} \tag{1.60}$$

and for small values of the exponent

$$X_r \simeq X_\infty\left(1 + \frac{2\gamma V_m}{RTr}\right) \tag{1.61}$$

Taking the following typical values: $\gamma = 200$ mJ m^{-2}, $V_m = 10^{-5}$ m^3, $R = 8.31$ J mol^{-1} K^{-1}, $T = 500$ K gives

$$\frac{X_r}{X_\infty} \simeq 1 + \frac{1}{r(\text{nm})}$$

e.g. for $r = 10$ nm $X_r/X_\infty \sim 1.1$. It can be seen therefore that quite large solubility differences can arise for particles in the range $r = 1$–100 nm. However, for particles visible in the light microscope ($r > 1$ μm) capillarity effects are very small.

1.7 Ternary Equilibrium

Since most commercial alloys are based on at least three components, an understanding of ternary phase diagrams is of great practical importance. The ideas that have been developed for binary systems can be extended to systems with three or more components[4].

The composition of a ternary alloy can be indicated on an equilateral triangle (the Gibbs triangle) whose corners represent 100% A, B or C as shown in Fig. 1.40. The triangle is usually divided by equidistant lines parallel to the sides marking 10% intervals in atomic or weight per cent. All points on lines parallel to BC contain the same percentage of A, the lines parallel to AC represent constant B concentration, and lines parallel to AB constant C concentrations. Alloys on PQ for example contain 60% A, on RS 30% B, and TU 10% C. Clearly the total percentage must sum to 100%, or expressed as mole fractions

$$X_A + X_B + X_C = 1 \tag{1.62}$$

The Gibbs free energy of any phase can now be represented by a vertical distance from the point in the Gibbs triangle. If this is done for all possible compositions the points trace out the free energy *surfaces* for all the possible phases, as shown in Fig. 1.41a. The chemical potentials of A, B and C in any phase are then given by the points where the *tangential plane* to the free energy surfaces intersects the A, B and C axes. Figure 1.41a is drawn for a

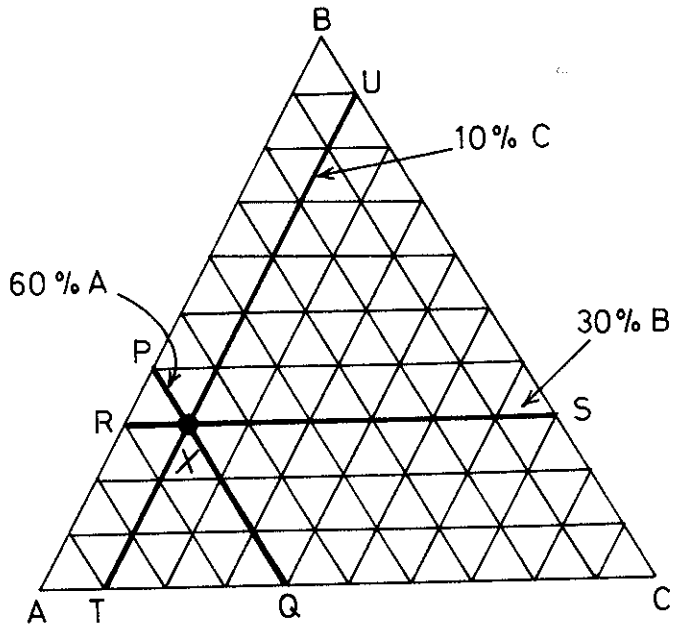

Fig. 1.40 The Gibbs triangle.

system in which the three binary systems AB, BC and CA are simple eutectics. Free energy surfaces exist for three solid phases α, β and γ and the liquid phase, L. At this temperature the liquid phase is most stable for all alloy compositions. At lower temperatures the G^L surface moves upwards and eventually intersects the G^α surface as shown in Fig. 1.41b. Alloys with compositions in the vicinity of the intersection of the two curves consist of α + L at equilibrium. In order for the chemical potentials to be equal in both

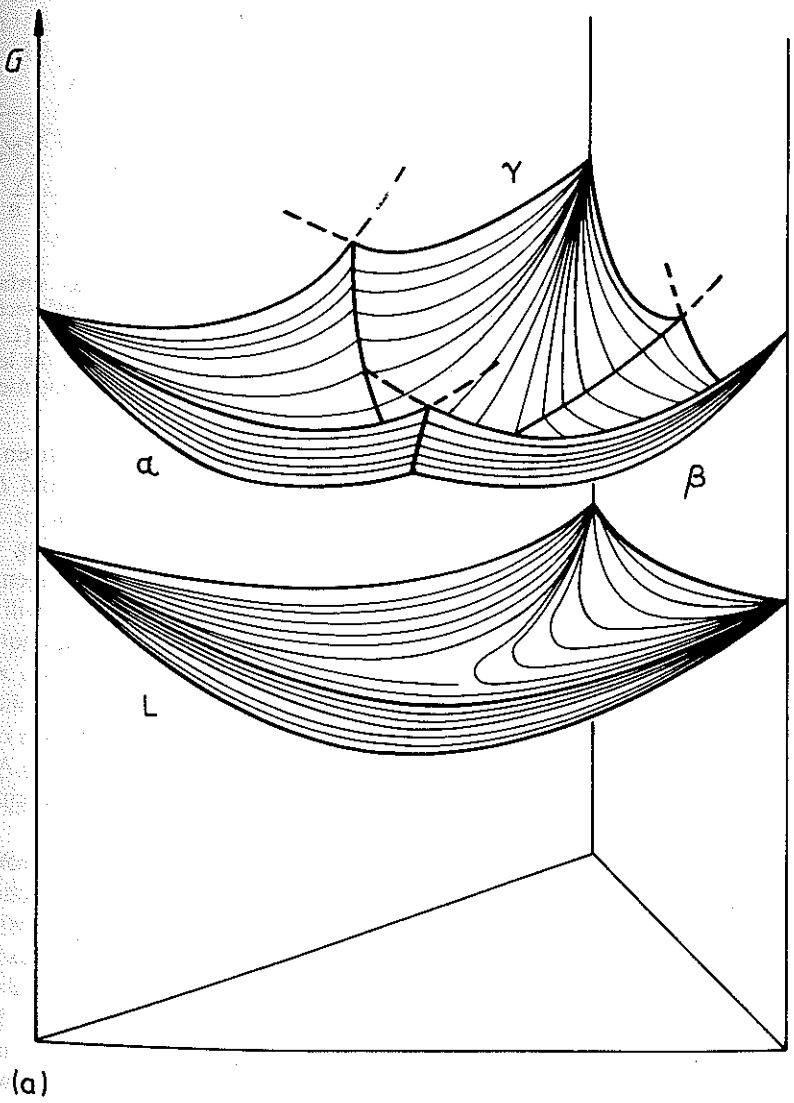

Fig. 1.41 (a) Free energies of a liquid and three solid phases of a ternary system.